

Adaptive Sparse ViT: Towards Learnable Adaptive Token Pruning by Fully Exploiting Self-Attention

Xiangcheng Liu^{1*}† Tianyi Wu^{2,3*} Guodong Guo^{2,3‡}

¹Peking University, Beijing, China

²Institute of Deep Learning, Baidu Research, Beijing, China

³National Engineering Laboratory for Deep Learning Technology and Application, Beijing, China
liuxiangcheng@stu.pku.edu.cn, wutianyi01@baidu.com, Guodong.Guo@mail.wvu.edu

Abstract

Vision transformer has emerged as a new paradigm in computer vision, showing excellent performance while accompanied by expensive computational cost. Image token pruning is one of the main approaches for ViT compression, due to the facts that the complexity is quadratic with respect to the token number, and many tokens containing only background regions do not truly contribute to the final prediction. Existing works either rely on additional modules to score the importance of individual tokens, or implement a fixed ratio pruning strategy for different input instances. In this work, we propose an adaptive sparse token pruning framework with a minimal cost. Our approach is based on learnable thresholds and leverages the Multi-Head Self-Attention to evaluate token informativeness with little additional operations. Specifically, we firstly propose an inexpensive attention head importance weighted class attention scoring mechanism. Then, learnable parameters are inserted in ViT as thresholds to distinguish informative tokens from unimportant ones. By comparing token attention scores and thresholds, we can discard useless tokens hierarchically and thus accelerate inference. The learnable thresholds are optimized in budget-aware training to balance accuracy and complexity, performing the corresponding pruning configurations for different input instances. Extensive experiments demonstrate the effectiveness of our approach. For example, our method improves the throughput of DeiT-S by 50% and brings only 0.2% drop in top-1 accuracy, which achieves a better trade-off between accuracy and latency than the previous methods.

Introduction

Recently, Vision Transformer (ViT) has made remarkable progress on image classification [5, 25, 16], object detection [1, 39], semantic segmentation [37, 30], and other vision tasks. However, as the model complexity is quadratic to the number of tokens, ViT suffers from expensive computational costs, which limits its application and deployment.

Not all image patches are helpful for the final prediction. For instance, the large number of image tokens in the background region do not contribute to the recognition and can be

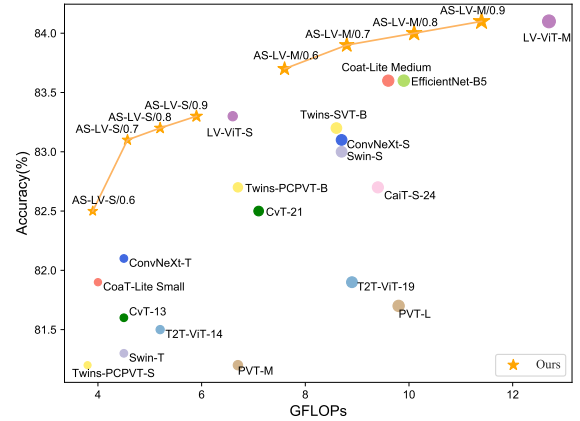


Figure 1: Trade-offs between complexity and top-1 accuracy for different models on ImageNet.

pruned during the inference process, greatly accelerating the model runtime without significant impact on performance. Token pruning has attracted the interests of many researchers. We classify the existing methods according to whether additional calculations are introduced to evaluate the token score. Evo-ViT [32] utilizes class attention [32] to estimate token score and develop a novel slow-fast token evolution approach to improve the throughput of ViT. EViT [14] employ a similar method to measure token importance and fuse discarded tokens. Both of these approaches require manually specifying the pruning ratio for each stage, and perform the same pruning policy for different input instances, which may result in simple samples being under-pruned or complex samples being over-pruned in the beginning stages, as illustrated in Figure 2 top. Another type of work identifies token importance via extra measures. DynamicViT [22] prune tokens in a fixed ratio by inserting lightweight predictors to predict token scores. IA-RED² [21] introduce a multi-head interpreter and employed reinforcement learning to generate pruning scheme for each token. A-ViT [34] compute halting scores for all tokens to adaptively discard unimportant tokens. The latter two achieve sample-adaptive token pruning at the cost of additional computation of significance scores for all tokens.

In this work, we propose an adaptive token sparse frame-

*Equal contribution

†Interns at the Institute of Deep Learning, Baidu Research

‡Corresponding author

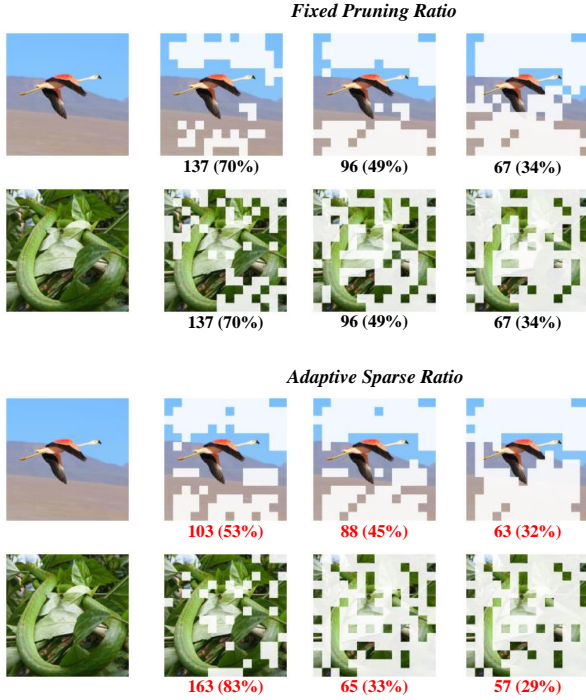


Figure 2: Comparison of fixed pruning rate (up) and adaptive sparse rate (down). The number denotes the amount and percentage of tokens kept in the current stage.

work for ViT acceleration, named AS-ViT, which fully exploits Multi-Head Self-Attention (MHSA) to estimate token importance scores, and uses a minimal cost, only three learnable thresholds, to perform the corresponding token pruning policy for a specific input instance as shown in Figure 2 bottom. Specifically, we first propose the attention head importance weighted class attention score. It uses the intermediate results of MHSA to calculate token-level head importance, which is then multiplied as a weighting factor on the class attention [32] score to better identify informative tokens. Then, we insert three learnable thresholds in ViT hierarchically. Only tokens with a score greater than the current threshold will be kept, and the pruned token will not participate in the later computations. Lastly, we propose a budget-aware loss to optimize the thresholds to achieve a trade-off between accuracy and computational effort across the dataset. During testing, the learnable threshold is fixed and we just compare the threshold and individual token scores to actually discard uninformative tokens for hardware acceleration. We investigate the intrinsic features of MHSA and reuse its computational results to evaluate the informativeness of the token. Threshold-based comparison avoids sorting all tokens. We minimize the computational cost of the proposed method with a combination of the two above approaches.

We conduct extensive token pruning experiments for the widely used vision transformer backbones, DeiT [25] and LV-ViT [11] on ImageNet. The experimental results demonstrate the effectiveness of our proposed adaptive dynamic token pruning method. For instance, our method improves 1.5x

throughput with only 0.2% decrease in accuracy while reducing the 35% GFLOPs of the DeiT-small model. For other model and pruning rates, our method also achieves a better accuracy and complexity balance compared with previous approaches.

Related Work

Vision Transformer. Transformer [27], developed in NLP, has been successfully applied to various vision tasks and tends to replace CNN [9, 23] gradually. ViT [5] illustrates that transformer lacks inductive bias and requires large-scale dataset pre-training to achieve an approximate performance with the state-of-the-art CNN. DeiT [25] eliminates the above problem with well-tuned training parameters and the introduction of distillation token. LV-ViT [11] explores a variety of techniques for training vision transformer, significantly improving the performance of ViT. PVT [28] constructs a hierarchical ViT similar to CNN and proposes spatial-reduction attention to reduce the computation complexity. Swin Transformer [16] proposes a window based self-attention that makes the complexity linear with respect to token number and becomes a generic visual backbone widely applicable to downstream tasks.

Static ViT Pruning. Analogous to weights pruning in CNN [8, 13, 20, 15, 18, 6], there are many works [38, 33, 2, 35] for ViT parameters compression. VTP [38] prunes parameters in MHSA and FFN indiscriminately through L1 regularized sparse training. NViT [33] establishes the global weights importance via performing Taylor expansion to the loss, then conducts structured pruning and parameter reassignment based on dimensional trends. SViT [2] fully explores the sparsity of ViT, compressing transformer with structured pruning, unstructured sparsity and token pruning. In this paper, we focus on token compression, which is orthogonal to static ViT pruning, and we can further improve the compression rate, benefit from weights pruning.

Dynamic ViT Pruning. Thanks to the transformer’s parallel computing mechanism, pruning image tokens can bring real acceleration without the need of additional support. Both DynamicViT [22] and IA-RED² [21] dynamically keep informative tokens by inserting prediction modules. PS-ViT [24] belongs to static token pruning, which statistically obtains the importance distribution of tokens across the dataset and prunes them top-down. EViT [14] and Evo-ViT [32] use the class attention score to distinguish how informative a token is. A-ViT [34] adaptively calculates the halting score for each token. Our method strives to implement instance-wise token pruning without additional computational costs.

Method

Preliminary

Vision Transformer [5] provides a new paradigm for image recognition. ViT first splits the image into $N \times N$ non-overlapping patches and embeds them into a D dimensional feature space, and then adds a class token before the image tokens for final classification. Considering the position relationship, all tokens are added with a learnable position

encoding and then fed into a stacked transformer block. We summarize the operations inside the block by using the following two equations:

$$x_{\text{MHSA}} = x + \text{MHSA}(\text{LN}(x)), \quad (1)$$

$$x_{\text{FFN}} = x_{\text{MHSA}} + \text{FFN}(\text{LN}(x_{\text{MHSA}})), \quad (2)$$

where MHSA stands for Multi-Head Self-Attention [27], FFN is feed-forward neural network, and LN stands for layer normalization.

MHSA represents features in multiple subspaces using the same parameters. The input is first projected into three matrices Query $\mathbf{Q} \in \mathbb{R}^{(N+1) \times D}$, Key $\mathbf{K} \in \mathbb{R}^{(N+1) \times D}$, and Value $\mathbf{V} \in \mathbb{R}^{(N+1) \times D}$, respectively, and then sliced into H attention heads to perform the parallel operations:

$$\text{Context}(\mathbf{Q}, \mathbf{K}, \mathbf{V}) = \text{Softmax}\left(\frac{\mathbf{Q}\mathbf{K}^T}{\sqrt{D_h}}\right) \mathbf{V}, \quad (3)$$

where $D_h = \frac{D}{H}$ is the feature dimension of the single head output. In particular, the attention scores of class token x_{cls} and other tokens can be written as:

$$\mathbf{A}(x_{\text{cls},:}) = \text{Softmax}\left(\frac{\mathbf{Q}_{\text{cls}}\mathbf{K}^T}{\sqrt{D_h}}\right) \in \mathbb{R}^{H \times N}, \quad (4)$$

which is used to reflect which tokens are contributing to the classification. Next, MHSA concatenates the Context of all attention heads together and project them through a matrix.

Class attention score weighted by attention head importance

Popular metrics for evaluating the importance of a token include its similarity score to the class token [14, 32] and the attention it receives from other tokens [7, 12]. However, we observed that both approaches ignore the diversity of attention heads, and the scores of different heads are treated equally, in other words, the final score is their average value.

Considering that different tokens may receive diverse attention in multiple attention heads, we propose a metric to estimate the token-level head importance, and it simply relies on the intermediate results of MHSA. Taking the i -th input token x_i as an example, firstly, we define the Context of the h -th head of the l -th layer as $\text{Context}^{(h,l)}(x_i) \in \mathbb{R}^{D_h}$, then we calculate the l_2 -norm along the feature dimension as the importance $\mathcal{H}^{(h,l)}(x_i)$ of the h -th head like Equation (5):

$$\mathcal{H}^{(h,l)}(x_i) = \sqrt{\sum_{j=1}^{D_h} \text{Context}_j^{(h,l)}(x_i)^2}. \quad (5)$$

Our motivation for estimating head importance derives from CNN pruning, of which l_2 -norm [10] is a commonly used metric for filter significance rating. In addition, our metrics are token-level, different from the previous head pruning work [19]. Next, we take the proportion of the importance rating of the h -th attention head to the sum of all head impor-

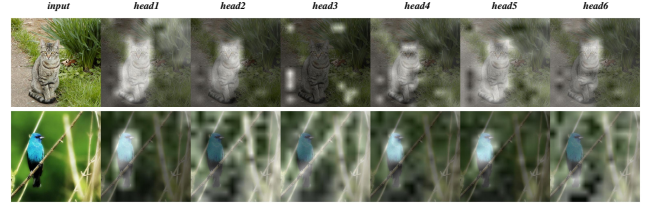


Figure 3: Visualization of tokens' attention paid to each head. The figure on the top is the token-level attention head importance visualization from AS-DeiT-S layer 7, and the figure below is from AS-DeiT-S layer 9.

tances as its weighting factor like Equation (6):

$$\mathcal{R}^{(h,l)}(x_i) = \frac{\mathcal{H}^{(h,l)}(x_i)}{\sum_{h=1}^H \mathcal{H}^{(h,l)}(x_i)}, \quad (6)$$

$$\mathcal{S}^l(x_i) = \sum_{h=1}^H \mathcal{R}^{(h,l)}(x_i) \cdot \mathbf{A}^{(h,l)}(x_{\text{cls},i}), \quad i = 1, 2, \dots, N. \quad (7)$$

We visualize the token-level head importance in the Figure 3 and brighter areas indicate that the current attention head is more important for this token. Taking the second image as an example, the tokens of foreground content focus more on head 1, 4 and 5, while the background area tokens clearly favor head 2 and 3. It is clear that the diversity of individual heads should be taken into account when scoring tokens.

The vanilla class attention score $\mathbf{A}^{(h,l)}(x_{\text{cls},i})$ of the i -th token is chosen as the basic evaluation metric, and we can estimate token score $\mathcal{S}^l(x_i)$ more accurately through head importance weighting as Equation (7). The flow of head importance weighted class attention score is shown in Figure 4. Compared to existing adaptive token pruning works, our approach takes into account the attention head diversity and has no reliance on any extra scoring mechanisms.

Adaptive token pruning based on learnable thresholds

In order to achieve sample-adaptive token pruning while minimizing the operation cost. We introduce three stage-wise learnable thresholds to control token sparse behavior, following LTP [12]. Figure 4 illustrates the overall framework of our proposed method. We usually divide the successive transformer blocks into four stages and insert a learnable threshold θ before the second, third and fourth stages, respectively. Adaptive Sparse Module is a comparator based on thresholds and token scores. We keep tokens with scores greater than the threshold, as in Equation (8):

$$M^n(x_i) = \begin{cases} 1, & \text{if } \mathcal{S}^l(x_i) > \theta^n \\ 0, & \text{otherwise} \end{cases}, \quad n = 1, 2, 3, \quad (8)$$

where $M^n(x_i)$ is a binary mask to indicate whether the i -th token is pruned or not, and $\mathcal{S}^l(x_i)$ denotes token score of the layer before the n -th stage. The token scores corresponding to different input images usually present different distributions,

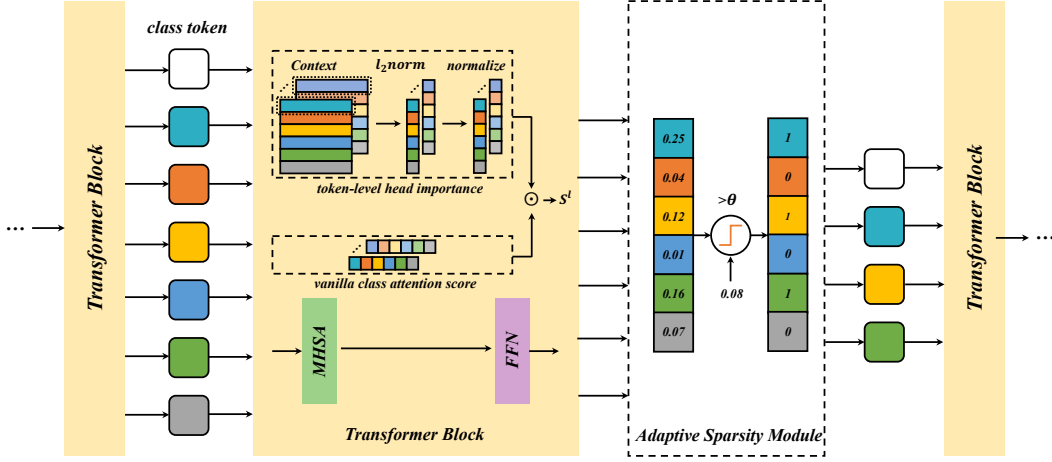


Figure 4: The framework of our Adaptive Sparse ViT. θ denotes the learnable threshold and \odot indicates Hadamard product. The token evaluation metric accounts for the attention of class token as well as the importance of different attention heads. Adaptive Sparse Module fulfills pruning by comparing token scores and thresholds.

so using a threshold to truncate the distribution can yield a specific pruning strategy for each instance.

Considering images in the same mini-batch have different pruning configurations, for the sake of parallel training, we cannot simply discard uninformative tokens during the training process. $M^n(x_i)$ can be used to explicitly cut the connection between uninformative tokens and useful tokens. There are two masking methods, attention mask [22] and activation mask [12], the former acting on the attention matrix and the latter on the output of the FFN.

However, it is not easy to optimize the learnable thresholds. The pruning mask comes from comparison, blocking the gradient back propagation, making the threshold untrained. We transform the hard mask into a soft differentiable mask using the sigmoid function:

$$\tilde{M}^n(x_i) = \text{Sigmoid}(T \cdot (S^l(x_i) - \theta^n)), \quad n = 1, 2, 3. \quad (9)$$

To approximate the hard mask, we employ a temperature parameter T , where the Sigmoid function behaves close to the step function at a sufficiently high temperature. The soft mask is differentiable, and by using the gradient straight through estimator (STE), we are able to optimize the learnable threshold as normal. A detailed implementation is given in the Appendix Listing 1.

Budget-aware Training

We achieve token pruning by constraining the target computation across the dataset. Compared to DynamicViT [22], which manually sets the token sparsity ratio at each stage to indirectly control the complexity, our method automatically achieves a good trade-off between accuracy and complexity given only a budget. Specifically, we propose a budget-aware loss ($\mathcal{L}_{\text{FLOPs}}$). Given a mini-batch inputs x with size of B , we can obtain their average FLOPs and then make the actual computational cost close to the target budget using MAE loss as Equation (10):

$$\mathcal{L}_{\text{FLOPs}} = \|\text{FLOPs}(x, \Theta) / B - t\|_1, \quad (10)$$

where FLOPs is a function to calculate the actual floating point operations for different inputs under the effect of all thresholds Θ , and t is the expected complexity. The original intention of designing the budget-aware loss is consistent with our sample-adaptive approach. The learnable thresholds are optimized to the appropriate range in a data-driven manner under the budget constraint, without imposing other artificial restrictions.

Our training objective include other two parts. The first part is the regular cross-entropy loss (\mathcal{L}_{CE}) as following equation:

$$\mathcal{L}_{\text{CE}} = \text{CrossEntropy}(y, \hat{y}) \quad (11)$$

where y denotes the ground truth labels and \hat{y} the Softmax output. To further improve the performance, we consider transferring the knowledge of the full model to the compressed network during training. Let the distribution \hat{y}_t denote the prediction of the teacher network, and we use KL divergence to minimize the gap between the output of the student network and the teacher network. For vision transformers like LV-ViT [11] with an additional linear layer to integrate all image tokens, it also needs to be aligned with the teacher network. Therefore, distillation loss ($\mathcal{L}_{\text{distill}}$) can be written as:

$$\mathcal{L}_{\text{distill}} = \text{KL}(\hat{y}, \hat{y}_t) \quad \text{or} \quad \mathcal{L}_{\text{distill}} = \text{KL}(\hat{y}, \hat{y}_t) + \text{KL}(\hat{z}, \hat{z}_t). \quad (12)$$

The overall training objective is a combination of the above three components:

$$\mathcal{L} = \mathcal{L}_{\text{CE}} + \lambda_1 \mathcal{L}_{\text{FLOPs}} + \lambda_2 \mathcal{L}_{\text{distill}}, \quad (13)$$

where λ is used to control the loss balance, and we set $\lambda_1 = 2$, $\lambda_2 = 0.5$ in our experiments.

Inference. Learnable thresholds are fixed after the training. Given an input image to do inference, we only need the intermediate result of MHSA to get the token score effortlessly. The pruning process is also simple enough that our

Table 1: Comparisons with the previous token pruning method on ImageNet. GFLOPs represents the average computational costs across the dataset.

Model	Params (M)	GFLOPs	Top-1 Acc (%)
DeiT-S [25]	22.1	4.6	79.8
DyViT [22]	22.8	2.9	79.3 (-0.5)
PS-ViT [24]	22.1	2.6	79.4 (-0.4)
IA-RED ² [21]	-	3.2	79.1 (-0.7)
Evo-ViT [32]	22.1	3.0	79.4 (-0.4)
EViT-DeiT-S [14]	22.1	3.0	79.5 (-0.3)
A-ViT [34]	22.1	3.6	78.6 (-1.2)
AS-DeiT-S (Ours)	22.1	3.0	79.6 (-0.2)
DyViT [22]	22.8	2.2	77.5 (-2.3)
EViT-DeiT-S [14]	22.1	2.3	78.5 (-1.3)
AS-DeiT-S (Ours)	22.1	2.3	78.7 (-1.1)
LV-ViT-S [11]	26.2	6.6	83.3
DyViT-LV-S [22]	26.9	4.6	83.0 (-0.3)
EViT-LV-S [14]	26.2	4.7	83.0 (-0.3)
AS-LV-S (Ours)	26.2	4.6	83.1 (-0.2)
DyViT-LV-S [22]	26.9	3.7	82.0 (-1.3)
EViT-LV-S [14]	26.2	3.9	82.5 (-0.8)
AS-LV-S (Ours)	26.2	3.9	82.6 (-0.7)
LV-ViT-M [11]	55.8	12.7	84.1
DyViT-LV-M [22]	57.1	9.6	83.9 (-0.2)
AS-LV-M (Ours)	55.8	9.6	84.0 (-0.1)
DyViT-LV-M [22]	57.1	8.5	83.8 (-0.3)
AS-LV-M (Ours)	55.8	8.5	83.9 (-0.2)

method only needs one comparison to know which tokens are to be kept, saving the topK computation cost compared to the previous work [22, 32, 14].

Experiments

Implementation details

Our experiments are conducted on the ImageNet-1K [4] classification dataset, with token pruning performed on the popular DeiT [25] and LV-ViT [11] models. We finetune the pre-trained model by 30 epoch to obtain the compressed network, and most of the training settings stay the same as the originals. More experiment details can be found in the Appendix.

Main results

Performance comparisons with existing pruning methods. We test the Top-1 accuracy, throughput and hardware latency of three models, DeiT-S [25], LVViT-S [11] and LVViT-M [11], under different pruning budgets and compare them with previous token pruning work [22, 14, 32, 24, 21]. The experimental results on accuracy are illustrated in Table 1. Compared to previous work, our proposed adaptive sparse ViT achieves state-of-the-art performance with similar complexities. For all models, the Top-1 accuracy degradation

Table 2: Effectiveness of each module.

Model	ASM	HS	Acc (%)	Throughput (img/s)
AS-DeiT-S		✓	79.36	1099
			79.36	1086
	✓	✓	79.56 (+0.2)	1198
	✓		79.63 (+0.27)	1192

Table 3: Effect of different masking strategies and distillation.

Method	Acc (%)	GFLOPs
+ attention_mask	79.63	3.0
+ activation_mask	78.04 (-1.59)	3.0
w/o $\mathcal{L}_{\text{distill}}$	79.46 (-0.17)	3.0

of our pruned models is controlled within 0.2% when the computation decreases by 30%~35%. When the compression rate of DeiT-small [25] is further increased to 50%, the advantage of sample-adaptive token sparsity becomes more obvious over the fixed pruning rate approaches [22, 14], as they may be forced to discard some important tokens. In addition, our method is far better than [21, 34], which are also sample-adaptive. It may be that the reinforcement learning strategy used by [21] is difficult to converge and requires iterative finetuning.

Efficiency comparisons with existing pruning methods.

The experimental results on efficiency are illustrated in Table 4. Note that we only compared with methods that have released the code and trained weights. Compared to previous work, AS-ViT achieves the best results in terms of accuracy, throughput and hardware latency. In contrast to methods like DynamicViT [22] that use extra modules to calculate token scores, AS-ViT relies only on the intermediate results of MHSA to evaluate tokens, thus saving expensive computations and achieving higher throughput metrics. Our method beats [32, 14] with sample-adaptive pruning and a more accurate token scoring mechanism. Moreover, the threshold-based comparator saves the computational cost of ranking all tokens, which makes our latency metrics significantly better than previous work.

Comparisons with other models. We compare the complexity and accuracy of our adaptive sparse LV-ViT (abbreviated as AS-LV-ViT) with other sota models on ImageNet in Figure 1. Detailed data and metrics such as throughput can be found in the Table 4. Our AS-LV-ViT shows quite competitive performance under different complexities, with far higher throughput than other CNN [23, 17] and ViT [16, 3, 28, 31, 29, 26, 11, 36] while still providing advanced accuracy. In addition, by simply adjusting the budget, our approach achieves a better accuracy-complexity trade-off compared automatically, avoiding the tedium and sub-optimality of manual design.

Table 4: Comparisons with the previous token pruning method on ImageNet. The throughput metric is measured on a single NVIDIA 2080Ti GPU using a fixed batch size 64 and hardware latency is the average elapsed time of 100 inferences with a single image on the same machine.

Model	Top-1 Acc (%)	Throughput (img/s)	Latency (ms)
DeiT-S [25]	79.8	770	6.16
DyViT [22]	79.3	1155 (+50%)	7.95 (+29%)
Evo-ViT [32]	79.4	1143 (+48%)	8.66 (+41%)
EViT-DeiT-S [14]	79.5	1149 (+49%)	7.3 (+19%)
AS-DeiT-S (Ours)	79.6	1192 (+55%)	6.56 (+6%)
EViT-DeiT-S [14]	78.5	1494 (+94%)	7.19 (+17%)
AS-DeiT-S (Ours)	78.7	1520 (+97%)	6.38 (+4%)
LV-ViT-M[11]	83.3	571	9.24
DyViT-LV-S [22]	83.0	807 (+41%)	11.06 (+20%)
AS-LV-S (Ours)	83.1	884 (+55%)	9.20 (-0%)
DyViT-LV-S [22]	82.0	1011 (+77%)	11.04 (+19%)
AS-LV-S (Ours)	82.6	1023 (+80%)	9.31 (+1%)
LV-ViT-M[11]	84.1	317	11.63
AS-LV-M (Ours)	84.0	657 (+107%)	11.43 (-2%)
DyViT-LV-M [22]	83.8	476 (+50%)	13.29 (+14%)
AS-LV-M (Ours)	83.9	801 (+153%)	11.53 (-1%)

Table 5: Comparison with the raw attention matrix of the pre-trained model.

	Method	$\rho=0.9$	$\rho=0.8$	$\rho=0.7$	$\rho=0.5$
pretrained	vanilla	79.77	79.24	78.51	73.72
pretrained	HS	79.79	79.29	78.51	73.78
finetuned	AS-ViT	79.8	79.7	79.6	78.7

Ablation Analysis

Effectiveness of each sub-module. In Table 2, we study the effect of each module in detail. **ASM** represents the Adaptive Sparsity Module, and **HS** is attention head importance weighted class attention score. In the ablation experiments, we use fixed ratio topK module instead of ASM and vanilla class attention score to replace HS. It is obvious that the Adaptive Sparsity module significantly improves the model performance compared with the fixed ratio module by 0.2%, which fully illustrates the necessity and effectiveness of sample adaptive token pruning. With ASM, the attention head weighted class attention score improves the precision by 0.07% compared to the original metric without a noticeable reduction in throughput. In addition, we can observe that HS needs to be used with ASM to have better results.

Effectiveness of training techniques. We apply masking strategy to achieve parallel training and knowledge distillation to stabilize the training process and improve accuracy. The respective experimental results are listed in Table 3. We

Table 6: Accuracy on ImageNet with different batch_size.

Batch Size	1	32	64	128
Acc (%)	79.63	79.60	79.58	79.61
GFLOPs	3.0	3.0	3.0	3.0

conduct experiments with DeiT-Small [25]. Obviously, attention_mask is far better than activation_mask, which can shield the uninformative tokens from interacting with other tokens. And by transferring the knowledge of full model to the compressed model, we can further improve the accuracy after pruning.

Comparison with raw attention baseline of pre-trained model. In this part, we consider the attention of the pre-trained model as a token evaluation metric and discard unimportant tokens in a fixed proportion. In addition, we apply head importance weighted class attention score (**HS**) directly on the raw attention baseline to fully demonstrate the effectiveness of our proposed method. The data in Table 5 present the ImageNet Top-1 accuracy for each method at different keeping rates. The attention map of the pre-trained model is no longer reliable and the accuracy decreases significantly as the compression ratio gradually increases. While our method can still achieve the similar performance of the original model by fine-tuning. In addition, our head importance weighted token score can produce positive results without training.

Batch Inference. Our approach achieves both sample-adaptive and batch-adaptive token pruning. The fact that AS-ViT is well suited for single-image computation scenarios does not mean that it cannot be used for parallel inference. Since we use the average complexity of mini-batch to calculate the budget-aware loss, we can also do parallel inference from the mean value of the number of kept tokens within a batch. And the experimental results in the Table 6 show that this does not cause significant accuracy degradation.

Performance on large model and different resolutions.

To fully demonstrate the effectiveness of our proposed method, we perform token sparse on the large baseline model DeiT-Base at different input resolutions. As illustrated in the Table 8, AS-ViT performs better than previous work under the same resolution and complexity. When using larger resolutions, our method is significantly better than IA-RED² [21]. Furthermore, at a resolution of 384x384, the accuracy degradation of AS-ViT is smaller compared to 224x224, suggesting that there is greater redundancy at higher resolutions, which can improve efficiency through token pruning.

Pruning location. Referring to previous works [22, 14], our approach adopts a progressive token sparse strategy. The position and number of our Adaptive Sparsity Module are also need to consider. We experiment with several insertion configurations to demonstrate that the current strategy is accuracy-latency optimal. The results such as accuracy and throughput are given in Table 7. The current method has higher accuracy compared to the [3,6,9] pruning strategy.

Table 7: Impacts of different module insertion configurations on accuracy and speed. We use the DeiT-small model with 65% FLOPs retained as the baseline.

Location	GFLOPs	Top-1 Acc (%)	Throughput (img/s)	Latency (ms)
[4, 7, 10]	3.0	79.63	1192	6.56
[3, 6, 9]	3.0	79.46	1184	6.54
[3, 5, 7, 9]	3.0	79.46	1191	6.60
[4, 6, 8, 10]	3.0	79.5	1195	6.65
[3, 4, ..., 10, 11]	3.0	78.8	1146	7.6

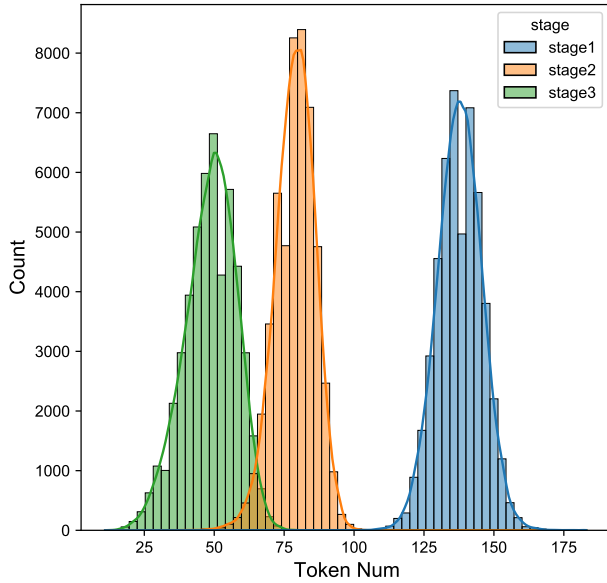


Figure 5: Distribution of the token number at different stages.

This may be attributed to the early layer’s class attention score not being stable enough, causing some information tokens to be discarded incorrectly. When increasing to 4 modules, there is no significant change in throughput and latency. We further insert trainable thresholds after the 3rd to 11th layers, respectively, and the training process becomes unstable and brings severe accuracy degradation, which we speculate is attributed to the difficulty of optimizing multiple thresholds in the limited fine-tuning. In addition, frequent reorganization of tokens causes non-negligible time consumption.

Visualization. To analyze the pruning behavior of our adaptive token sparse method on different images, we count the amount of maintained tokens by the AS-DeiT-S/ $f=0.65$ model in each stage for all images of the ImageNet [4] validation dataset and plot their distribution in Figure 5. The number of each stage basically shows a Gaussian distribution, peaking at a certain value. This suggests that a fixed proportion of pruning is also relatively reasonable, since the easy and difficult samples are only a minority. However, our adaptive token sparse method can give the corresponding pruning configurations for samples with different recognition difficulties, which is reflected in the distribution extending

Table 8: Experimental results of token pruning in large model and at different input resolutions.

Method	Resolution	Acc (%)	GFLOPs
DeiT-B [25]	224	81.8	17.5
DyViT-B [22]	224	81.3 (-0.5)	11.2
EViT-DeiT-B [14]	224	81.3 (-0.5)	11.5
IA-RED2 [21]	224	80.3 (-1.5)	11.8
AS-DeiT-B	224	81.4 (-0.4)	11.2
DeiT-B [25]	384	82.9	49.4
IA-RED2 [21]	384	81.9 (-1.0)	34.7
AS-DeiT-B	384	82.7 (-0.2)	34.6

to both sides. Further, we select three representative images for visualization of token pruning results. The three images shown in Figure 6 are the easy, normal and hard input samples for the model. For easy samples, AS-ViT discards plenty of useless tokens in the early stage to save computational cost, While for complicated and hard to recognize instances, the model tends to prune more tokens in later stages with higher confidence and discard a small number of tokens in the early phases. More image token pruning results can be found in the Appendix Figure 7.

Conclusion

In this work, we propose a sample-adaptive token pruning method, which effortlessly evaluates token importance via fully exploiting the MHSA mechanism, and then introduces learnable thresholds to accomplish pruning by comparing with token scores. Our proposed budget-aware loss can effectively constrain the thresholds so that the pruned model reaches the complexity budget while achieving a good accuracy-speed trade-off. Compared to previous work, our approach does not require additional sub-networks to compute token scores and also performs specific pruning strategies for different samples just by comparing with thresholds. Experimental results on various models show that our AS-ViT greatly improves the throughput and achieves lower latency without significantly affecting the accuracy. In the future, we will transfer token pruning to downstream tasks and combining it with static parameters pruning for further acceleration.

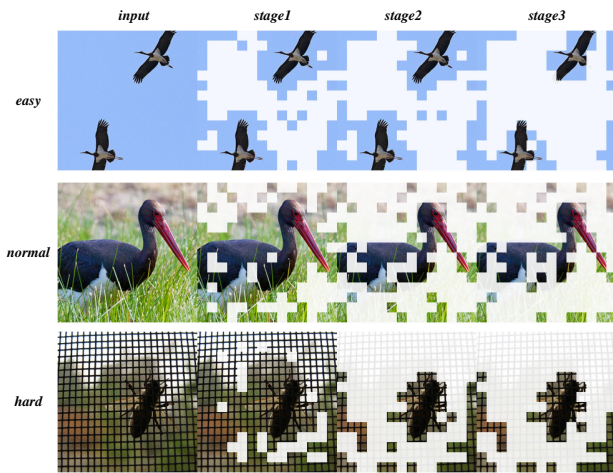


Figure 6: Visualization results of token pruning for samples with different recognition difficulties.

References

- [1] Carion, N.; Massa, F.; Synnaeve, G.; Usunier, N.; Kirillov, A.; and Zagoruyko, S. 2020. End-to-end object detection with transformers. In *ECCV*, 213–229. [1](#)
- [2] Chen, T.; Cheng, Y.; Gan, Z.; Yuan, L.; Zhang, L.; and Wang, Z. 2021. Chasing sparsity in vision transformers: An end-to-end exploration. *Advances in Neural Information Processing Systems*, 34. [2](#)
- [3] Chu, X.; Tian, Z.; Wang, Y.; Zhang, B.; Ren, H.; Wei, X.; Xia, H.; and Shen, C. 2021. Twins: Revisiting the design of spatial attention in vision transformers. *Advances in Neural Information Processing Systems*, 34. [5](#), [11](#)
- [4] Deng, J.; Dong, W.; Socher, R.; Li, L.-J.; Li, K.; and Fei-Fei, L. 2009. Imagenet: A large-scale hierarchical image database. In *CVPR*, 248–255. [5](#), [7](#)
- [5] Dosovitskiy, A.; Beyer, L.; Kolesnikov, A.; Weissenborn, D.; Zhai, X.; Unterthiner, T.; Dehghani, M.; Minderer, M.; Heigold, G.; Gelly, S.; et al. 2020. An Image is Worth 16x16 Words: Transformers for Image Recognition at Scale. In *International Conference on Learning Representations (ICLR)*. [1](#), [2](#)
- [6] Frankle, J.; and Carbin, M. 2018. The Lottery Ticket Hypothesis: Finding Sparse, Trainable Neural Networks. In *International Conference on Learning Representations*. [2](#)
- [7] Goyal, S.; Choudhury, A. R.; Raje, S.; Chakaravarthy, V.; Sabharwal, Y.; and Verma, A. 2020. PoWER-BERT: Accelerating BERT inference via progressive word-vector elimination. In *International Conference on Machine Learning*, 3690–3699. PMLR. [3](#)
- [8] Han, S.; Mao, H.; and Dally, W. J. 2015. Deep compression: Compressing deep neural networks with pruning, trained quantization and huffman coding. *arXiv preprint arXiv:1510.00149*. [2](#)
- [9] He, K.; Zhang, X.; Ren, S.; and Sun, J. 2016. Deep residual learning for image recognition. In *CVPR*, 770–778. [2](#)
- [10] He, Y.; Kang, G.; Dong, X.; Fu, Y.; and Yang, Y. 2018. Soft filter pruning for accelerating deep convolutional neural networks. *arXiv preprint arXiv:1808.06866*. [3](#)
- [11] Jiang, Z.; Hou, Q.; Yuan, L.; Zhou, D.; Shi, Y.; Jin, X.; Wang, A.; and Feng, J. 2021. All Tokens Matter: Token Labeling for Training Better Vision Transformers. *arXiv preprint arXiv:2104.10858*. [2](#), [4](#), [5](#), [6](#), [10](#)
- [12] Kim, S.; Shen, S.; Thorsley, D.; Gholami, A.; Kwon, W.; Hassoun, J.; and Keutzer, K. 2021. Learned token pruning for transformers. *arXiv preprint arXiv:2107.00910*. [3](#), [4](#)
- [13] Li, H.; Kadav, A.; Durdanovic, I.; Samet, H.; and Graf, H. P. 2016. Pruning filters for efficient convnets. *arXiv preprint arXiv:1608.08710*. [2](#)
- [14] Liang, Y.; GE, C.; Tong, Z.; Song, Y.; Wang, J.; and Xie, P. 2022. EviT: Expediting Vision Transformers via Token Reorganizations. In *International Conference on Learning Representations (ICLR)*. [1](#), [2](#), [3](#), [5](#), [6](#), [7](#), [10](#)
- [15] Liu, Z.; Li, J.; Shen, Z.; Huang, G.; Yan, S.; and Zhang, C. 2017. Learning Efficient Convolutional Networks through Network Slimming. In *ICCV*. [2](#)
- [16] Liu, Z.; Lin, Y.; Cao, Y.; Hu, H.; Wei, Y.; Zhang, Z.; Lin, S.; and Guo, B. 2021. Swin transformer: Hierarchical vision transformer using shifted windows. In *Proceedings of the IEEE/CVF International Conference on Computer Vision (ICCV)*, 10012–10022. [1](#), [2](#), [5](#), [11](#)
- [17] Liu, Z.; Mao, H.; Wu, C.-Y.; Feichtenhofer, C.; Darrell, T.; and Xie, S. 2022. A ConvNet for the 2020s. *Proceedings of the IEEE/CVF Conference on Computer Vision and Pattern Recognition (CVPR)*. [5](#), [11](#)
- [18] Luo, J.-H.; Wu, J.; and Lin, W. 2017. Thinet: A filter level pruning method for deep neural network compression. In *Proceedings of the IEEE international conference on computer vision*, 5058–5066. [2](#)
- [19] Michel, P.; Levy, O.; and Neubig, G. 2019. Are sixteen heads really better than one? *Advances in neural information processing systems*, 32. [3](#)
- [20] Molchanov, P.; Tyree, S.; Karras, T.; Aila, T.; and Kautz, J. 2016. Pruning convolutional neural networks for resource efficient inference. *arXiv preprint arXiv:1611.06440*. [2](#)
- [21] Pan, B.; Panda, R.; Jiang, Y.; Wang, Z.; Feris, R.; and Oliva, A. 2021. IA-RED²: Interpretability-Aware Redundancy Reduction for Vision Transformers. In *Advances in Neural Information Processing Systems (NeurIPS)*. [1](#), [2](#), [5](#), [6](#), [7](#)
- [22] Rao, Y.; Zhao, W.; Liu, B.; Lu, J.; Zhou, J.; and Hsieh, C.-J. 2021. DynamicViT: Efficient Vision Transformers with Dynamic Token Sparsification. In *Advances in Neural Information Processing Systems (NeurIPS)*. [1](#), [2](#), [4](#), [5](#), [6](#), [7](#)
- [23] Tan, M.; and Le, Q. 2019. Efficientnet: Rethinking model scaling for convolutional neural networks. In *ICML*, 6105–6114. PMLR. [2](#), [5](#), [11](#)

- [24] Tang, Y.; Han, K.; Wang, Y.; Xu, C.; Guo, J.; Xu, C.; and Tao, D. 2021. Patch slimming for efficient vision transformers. *arXiv preprint arXiv:2106.02852*. 2, 5
- [25] Touvron, H.; Cord, M.; Douze, M.; Massa, F.; Sablayrolles, A.; and Jégou, H. 2021. Training data-efficient image transformers & distillation through attention. In *International Conference on Machine Learning (ICML)*, 10347–10357. 1, 2, 5, 6, 7, 10, 11
- [26] Touvron, H.; Cord, M.; Sablayrolles, A.; Synnaeve, G.; and Jégou, H. 2021. Going deeper with image transformers. *arXiv preprint arXiv:2103.17239*. 5, 11
- [27] Vaswani, A.; Shazeer, N.; Parmar, N.; Uszkoreit, J.; Jones, L.; Gomez, A. N.; Kaiser, L.; and Polosukhin, I. 2017. Attention is all you need. In *NeurIPS*, 5998–6008. 2, 3
- [28] Wang, W.; Xie, E.; Li, X.; Fan, D.-P.; Song, K.; Liang, D.; Lu, T.; Luo, P.; and Shao, L. 2021. Pyramid vision transformer: A versatile backbone for dense prediction without convolutions. In *Proceedings of the IEEE/CVF International Conference on Computer Vision (ICCV)*, 568–578. 2, 5, 11
- [29] Wu, H.; Xiao, B.; Codella, N.; Liu, M.; Dai, X.; Yuan, L.; and Zhang, L. 2021. Cvt: Introducing convolutions to vision transformers. In *Proceedings of the IEEE/CVF International Conference on Computer Vision*, 22–31. 5, 11
- [30] Xie, E.; Wang, W.; Yu, Z.; Anandkumar, A.; Alvarez, J. M.; and Luo, P. 2021. SegFormer: Simple and Efficient Design for Semantic Segmentation with Transformers. *arXiv preprint arXiv:2105.15203*. 1
- [31] Xu, W.; Xu, Y.; Chang, T.; and Tu, Z. 2021. Co-scale conv-attentional image transformers. In *Proceedings of the IEEE/CVF International Conference on Computer Vision*, 9981–9990. 5, 11
- [32] Xu, Y.; Zhang, Z.; Zhang, M.; Sheng, K.; Li, K.; Dong, W.; Zhang, L.; Xu, C.; and Sun, X. 2022. Evo-ViT: Slow-Fast Token Evolution for Dynamic Vision Transformer. In *Proceedings of the AAAI Conference on Artificial Intelligence (AAAI)*. 1, 2, 3, 5, 6
- [33] Yang, H.; Yin, H.; Molchanov, P.; Li, H.; and Kautz, J. 2021. Nvit: Vision transformer compression and parameter redistribution. *arXiv preprint arXiv:2110.04869*. 2
- [34] Yin, H.; Vahdat, A.; Alvarez, J.; Mallya, A.; Kautz, J.; and Molchanov, P. 2021. AdaViT: Adaptive Tokens for Efficient Vision Transformer. *arXiv preprint arXiv:2112.07658*. 1, 2, 5
- [35] Yu, S.; Chen, T.; Shen, J.; Yuan, H.; Tan, J.; Yang, S.; Liu, J.; and Wang, Z. 2022. Unified Visual Transformer Compression. *arXiv preprint arXiv:2203.08243*. 2
- [36] Yuan, L.; Chen, Y.; Wang, T.; Yu, W.; Shi, Y.; Jiang, Z.-H.; Tay, F. E.; Feng, J.; and Yan, S. 2021. Tokens-to-Token ViT: Training Vision Transformers From Scratch on ImageNet. In *Proceedings of the IEEE/CVF International Conference on Computer Vision (ICCV)*, 558–567. 5, 11
- [37] Zheng, S.; Lu, J.; Zhao, H.; Zhu, X.; Luo, Z.; Wang, Y.; Fu, Y.; Feng, J.; Xiang, T.; Torr, P. H.; and Zhang, L. 2021. Rethinking Semantic Segmentation from a Sequence-to-Sequence Perspective with Transformers. In *CVPR*. 1
- [38] Zhu, M.; Tang, Y.; and Han, K. 2021. Vision Transformer Pruning. *arXiv preprint arXiv:2104.08500*. 2
- [39] Zhu, X.; Su, W.; Lu, L.; Li, B.; Wang, X.; and Dai, J. 2020. Deformable DETR: Deformable Transformers for End-to-End Object Detection. *arXiv preprint arXiv:2010.04159*. 1

Experiment details

We adopt the same fine-tuning strategy as EViT [14], and set the initial learning rate to $2e-5$ and decrease to $2e-6$ as cosine, while the weight decay is set to $1e-6$. For DeiT [25], we insert learnable thresholds after the 4th, 7th and 10th layers. For LV-ViT [11], we insert thresholds after the 5th, 9th, and 13th layers. We empirically set the temperature parameter T of the sigmoid function used to generate the soft binary pruning mask to $1e+4$. For all models, the initialized values of learnable thresholds are set to $[0.001, 0.002, 0.003]$.

Visualization

We obtained all pruning configurations for the AS-DeiT-S/ $f=0.65$ model on the ImageNet validation dataset and ranked them by the first stage’s token number. Then select the images that are easy, normal and complicated for our model and visualize their pruning effects. As shown in the Figure 7, our method prunes large numbers of uninformative tokens early for simple samples to save computational effort, uses the regular strategy for ordinary samples, and gradually increases the pruning rate for complex samples to ensure the recognition accuracy.

More Analysis

Comparisons with other models. We compare the complexity and accuracy of our adaptive sparse LV-ViT (abbreviated as AS-LV-ViT) with other sota models on ImageNet in Table 11.

Comparison with random baseline. We compare our method with a random and minimal baseline based on the pruning ratios obtained from adaptive pruning. The pruning ratio was first obtained by comparing the trained threshold with the token scores, and then two scenarios were experimented with randomly sampled tokens (random) and the lowest scoring k tokens (minK). The results in the Table 9 demonstrate the effectiveness of our method. The minK method discards a large number of information tokens, causing significant accuracy degradation, while random baselines perform moderately well at low compression rates and show obvious accuracy drop when the compression rate is increased. In contrast, our method retains the most informative tokens and achieves a precision-speed balance.

Effect of random seeds. We tried four random seeds in the DeiT-S model and the experimental results are shown in the Table 10, indicating that our method is stable.

Table 9: Results of the random baseline.

Method	GFLOPs	Acc (%)
minK	3.0	51.63
random	3.0	72.79
ours	3.0	79.63
minK	2.3	26.65
random	2.3	62.67
ours	2.3	78.70

Table 10: Accuracy under different random seeds.

seed	s1	s2	s3	s4
Acc (%)	79.63	79.60	79.57	79.62

Listing 1: Adaptive Sparsity Module in a PyTorch-like style.

```

1 # score: token score
2 # thres: learnable threshold
3 # tau: temperature parameter
4 # training: training/inference mode
5
6 def asm(score, thres, tau=1, training=
    False):
7     # batch size
8     B = score.size(0)
9     # inference mode
10    if not training:
11        idx = logits > thres
12        if B==1:
13            return idx
14        k = idx.sum().item() // B
15        return k
16
17    # training mode
18    y_soft = torch.sigmoid((score - thres)
        * tau)
19    y_hard = (y_soft > 0.5).float()
20    # straight through
21    mask = y_hard - y_soft.detach() +
        y_soft
22
23    return mask

```

Table 11: Comparisons of model complexity and accuracy on ImageNet with advanced CNN and ViT models. Throughput and latency are measured on the same machine.

Model	Params (M)	GFLOPs	Top-1 Acc (%)	Throughput (img/s)	Latency (ms)
DeiT-S [25]	22.1	4.6	79.8	770	6.16
PVT-S [28]	24.5	3.8	79.8	558	12.10
Twins-PCPVT-S [3]	24.1	3.8	81.2	557	11.54
CoaT-Lite Small [31]	19.8	4.0	81.9	368	15.68
Swin-T [16]	29.0	4.5	81.3	533	8.83
CvT-13 [29]	20.0	4.5	81.6	527	15.0
ConvNeXt-T [17]	28.6	4.5	82.1	332	5.39
T2T-ViT-14 [36]	22.0	5.2	81.5	601	8.78
AS-LV-S/0.6 (Ours)	26.2	3.9	82.6	1023	9.31
PVT-M [28]	44.2	6.7	81.2	362	19.49
Twins-PCPVT-B [3]	43.8	6.7	82.7	347	19.9
CvT-21 [29]	32.0	7.1	82.5	340	25.10
Twins-SVT-B [3]	56.1	8.6	83.2	313	16.15
ConvNeXt-S [17]	50.2	8.7	83.1	192	9.94
Swin-S [16]	49.6	8.7	83.0	308	17.0
T2T-ViT-19 [36]	39.2	8.9	81.9	375	11.66
CaiT-S-24 [26]	46.9	9.4	82.7	245	18.68
PVT-L [28]	61.4	9.8	81.7	249	28.3
CoaT-Lite Medium [31]	19.8	9.6	83.6	368	15.68
EfficientNet-B5*/456 [23]	30.0	9.9	83.6	97	17.51
AS-LV-M/0.67 (Ours)	55.8	8.5	83.9	801	11.53



Figure 7: Effects of token pruning for different difficulty images at three stages. Easy, normal and complicated samples are shown in order from top to bottom, separated by blank lines. Easy samples are discarded with lots of uninformative tokens in the first stage by our model, and the pruning rate of common samples gradually increases in each stage. Complex samples are pruned with only limited number of tokens in the initial stage, and useless tokens are discarded in the later stages as the confidence of the model increases.